Molecular Catalysis 560 (2024) 114128

Contents lists available at ScienceDirect

Molecular Catalysis

journal homepage: www.journals.elsevier.com/molecular-catalysis

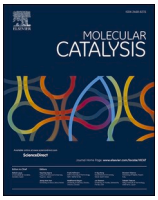

# Chitosan-supported calcium hydroxide hybrid material as new, efficient, and recyclable catalyst for biodiesel production

A. Aloia [a,1], M. Izzi [a,1], A. Rizzuti [b], M. Casiello [a,c], P. Mastrorilli [b], N. Cioffi [a], A. Nacci [a], R. A. Picca [a,*], A. Monopoli [a,*]

[a] Dipartimento di Chimica, Università degli Studi di Bari Aldo Moro, Via E. Orabona 4, 70125 Bari, Italy
[b] Dipartimento di Ingegneria Civile, Ambientale, del Territorio, Edile e di Chimica – DICATECh, Via Edoardo Orabona, 4 - 70125 Bari, Italy
[c] Istituto dei Composti Organometallici, ICCOM, C.N.R., c/o Dipartimento di Chimica, Università degli Studi di Bari Aldo Moro, Via E. Orabona 4, 70125 Bari, Italy

ARTICLE INFO

*Keywords:*
Biodiesel
Chitosan
Ca-based catalyst
XPS
FTIR
SEM-EDS

ABSTRACT

In this work, a novel supported catalyst was prepared starting from calcium chloride and chitosan flakes using a very mild approach in an aqueous medium without final calcination at high temperatures. The as-prepared catalyst was fully characterized by thermogravimetric analysis (TGA), attenuated total reflectance Fourier transform infrared (ATR-FTIR), and X-ray photoelectron (XPS) spectroscopies, transmission and scanning electron microscopies (TEM, SEM), Energy Dispersive X-ray Spectroscopy (EDS), demonstrating that it consists of calcium hydroxide particles of about 200 nm supported on chitosan micrometric structures. The most crucial parameters in the transesterification process were investigated. A methanol/oil ratio of 6:1, a reaction time of 6 h, and a temperature of 60 °C were found to lead to complete conversion. A reaction on a gram scale using waste oil as a starting material was also tested, and excellent results were achieved. Moreover, the catalyst proved to be very robust, since even after the 10th recycle, the conversion rate remained at around 90 %. Spectroscopic analyses showed minimal leaching of material without modification of chemical composition. The kinetic behavior (activation energy, $E_a$) of the catalyst was also studied, which resulted in similar outcomes to Ca-based systems present in the literature, but without the need for costly preparations and with superior recycling resistance. An $E_a$ value of 63.25 kJ·mol$^{-1}$ was found, which agrees with data reported in the literature.

## 1. Introduction

The encouraged energy transition needs "fuel" to move forward. It may seem like a contradiction, but the continued and growing demand for fuel from emerging and growing economies such as India, China, and African countries, instead of accelerating toward a green energy transition, increases demand for and consumption of fossil fuels, driving up prices of conventional energy sources [1].

However, the green transition must progress, so much so that the European Union has set a target of achieving a renewable energy share in transportation of at least 14 percent, including a minimum 3.5 percent share of advanced biofuels, by 2030 [2,3].

In this context, biofuels can be crucial in achieving the right energy supply mix. Among them, fatty acid methyl esters (FAMEs) are certainly the most studied, being ideal substitutes of petro-diesel as they can be used without any engine modification, giving also reduction of emissions of SOx, NOx, particulate matter, dangerous aromatic compounds, and sulfur derivatives into the environment [4]. The major drawbacks of biodiesel production are the threatening of food storages, due to the lands use changes, the high energy costs of the transesterification process and the use of strongly acidic or alkaline homogeneous catalysts, often employed under stoichiometric conditions and hard to be recycled [5].

In this sense, the discovery of heterogeneous, bio-based catalysts may be critical to making the whole process feasible and industrially attractive. To this end, an impressive number of papers have been published in recent years, and a wide variety of catalysts have been used [6–11], including titanium [12], zirconium [13] and zinc oxides [14,15], alumina [16–18], and also zeolites [19,20], just to cite a few.

Recently, some of us have published few works on this topic [21–24], in which steel slag [22] or multifunctional halloysite and hectorite [21,23] were used as efficient catalysts in biodiesel production [25].

* Corresponding authors.
*E-mail addresses:* rosaria.picca@uniba.it (R.A. Picca), antonio.monopoli@uniba.it (A. Monopoli).
[1] These authors contributed equally to the work as first authors.

https://doi.org/10.1016/j.mcat.2024.114128
Received 2 January 2024; Received in revised form 29 March 2024; Accepted 7 April 2024
Available online 12 April 2024
2468-8231/© 2024 The Authors. Published by Elsevier B.V. This is an open access article under the CC BY-NC-ND license (http://creativecommons.org/licenses/by-nc-nd/4.0/).

However, the Ca-based catalysts still are the most promising, since they are robust, inexpensive, safe, and with low solubility in methanol. Among them, CaO is the most studied, due to its high basicity, reactivity, and very low cost [9,10,26–32]. Calcium oxide is generally obtained through the decarbonation of limestone or other sources of $CaCO_3$ [33], including various shells [34] and even wasted eggshells [28,35–39]. Calcium hydroxide ($Ca(OH)_2$, hydrated lime) can also be used as a precursor of CaO [40]. As an example, in 2016, Promarak et al. prepared a low-cost CaO catalyst derived from hydrated lime, achieving high yields in FAMEs in 2 h. The catalyst was also recycled several times, with a loss of activity after 5 runs [41]. The transformation of calcium oxide into calcium carbonate, due to the reaction with $CO_2$, and into calcium hydroxide, attributable to the presence of water, were two of the identified reasons for the lower reactivity [42]. This last point represents an important disadvantage of the use of calcium oxide, specifically its sensitivity to moisture, which is often present in wasted oils: a few minutes are sufficient to chemisorb a significant amount of $H_2O$ (and also $CO_2$) [30].

As a matter of fact, starting from calcium hydroxide or carbonate [43] always requires a time-consuming, costly, and energy-intensive high-temperature calcination process to obtain CaO particles. In an attempt to bypass this tedious step, an alternative would be the use of calcium hydroxide directly. On the other hand, Granados et al. in 2007 showed that, in the case of calcium oxide, the surface of the activated catalyst is best described as an inner core of CaO particles covered by very few layers of $Ca(OH)_2$ [42].

Notwithstanding these findings, very few papers dealing with the direct application of $Ca(OH)_2$ in the transesterification reaction are reported in the literature, despite very good results [44–46]. Among them, no paper addressed the use of supported $Ca(OH)_2$ to preserve catalyst life and increase the number of recycles.

Chitosan is an affordable and nontoxic biopolymer obtained by the deacetylation of chitin, used in the agrochemical, food, and pharmaceutical industries. Its use in heterogeneous catalysis is promoted by its easy and clean elimination by incineration (or dissolution in acidic aqueous solutions), which can permit quantitative metal recovery [47]. Due to its strong affinity for calcium [48,49], chitosan has been used as a ligand in several composites. Fu et al. in 2011 utilized immobilized CaO on chitosan beads cross-linked with glutaraldehyde. The composite proved to be effective in biodiesel production (97 % conversion). The immobilized catalyst was also reused at least five times [50]. In 2014, some authors reported the use of chitosan-cryogel in the (trans)esterification of triolein and soybean oil with methanol, obtaining up to 90 % biodiesel (FAMEs) in 8–32 h at 100–150 °C. However, the recycling of chitosan beads was poor and required washing with *tert*-butanol and methanol to desorb fats and glycerol [51].

In addition, chitosan is claimed to have the ability to "bind" water and fatty substances (in some papers it is called fat-binding capacity), particularly triglycerides and free fatty acids [52], and this property may be an advantage to be evaluated in transesterification reactions of vegetable oils [53–57].

Following these findings, we propose here the synthesis and characterization of sub-micrometric particles of calcium hydroxide supported on chitosan, together with their use in the FAMEs production from soybean oil and wasted cooking oil (WCO).

## 2. Experimental

### 2.1. Materials

Calcium chloride ($CaCl_2$ > 99 % pur. p.a.), Chitosan (average molecular weight, degree of deacetylation 75–85 %), Sodium hydroxide (NaOH> 98 % pur. p.a, ACS), and glacial acetic acid were purchased from Merck-Sigma Aldrich. Milli-Q water was used for preparing solutions (25 °C; 18.2 mΩ•cm). Commercial soybean oil was from Valsoia S. p.A. Bologna, Italy. The fatty acid composition consists of palmitic acid 10.35 %, stearic acid 4.45 %, oleic acid 22.60 %, linoleic acid 30.95 %, linolenic acid 6.84 %, cis-11-eicosanoic acid 3.1 %, behenic acid 0.36 %, arachidic acid 0.36 %, others 1 %.

Waste cooking oil was a domestic source. Composition is reported in Supporting Information.

### 2.2. Synthesis of $Ca(OH)_2$/chitosan supported catalyst (Ca@CS)

$Ca(OH)_2$/chitosan catalyst was prepared following an easy and mild one-step protocol developed in our laboratories. Specifically, the alkaline precipitation of $Ca(OH)_2$ sub-micrometric particles was directly carried out in a chitosan solution forming a hybrid material consisting of the two components. Briefly, chitosan ($2\%_{w/v}$) was solubilized in 50 mL of $1\%_{v/v}$ acetic acid at 50 °C for 2 h. A proper amount of $CaCl_2$ was then added up to a final concentration of 0.2 M. The solution was stirred overnight at room temperature. Afterwards, 20 mL of NaOH 2.5 M was added dropwise, providing the immediate precipitation of $Ca(OH)_2$ and chitosan as Ca@CS. The process was performed at 80 °C under continuous stirring for 1 h [58]. The precipitate was washed with water under vacuum using a Büchner funnel until neutrality of the eluate and kept in an oven at 80 °C until complete drying. The resulting material in the form of chips was then crushed in a mortar obtaining a fine powder for further processing and use.

In a similar way, free $Ca(OH)_2$ submicrometric particles were also prepared, starting from a solution of 0.2 M aqueous $CaCl_2$.

### 2.3. Catalyst characterization

The catalyst was analyzed by FTIR, before and after use, in transmission mode with ATR diamond crystal with a Perkin Elmer Spectrum Two apparatus. 16 scans were acquired in the range 4000–400 $cm^{-1}$ (spectral resolution of 2 $cm^{-1}$). Thermogravimetric analyses (TGA) and simultaneous differential scanning calorimetry (DSC) measurements were performed in nitrogen or air flow (100 mL $min^{-1}$) with a TA instrument SDT Q600 thermal analyzer in the range from 30 °C to 1000 °C with a heating rate of 10 °C $min^{-1}$. XPS analysis was also performed on freshly prepared and used Ca@CS powders using a PHI Versaprobe II spectrometer with a monochromatized Al Kα source (200 μm spot size) under constant charge neutralization on at least three points per sample. Both survey and high-resolution spectra were acquired and then processed by Multipak software (v. 9.9.3). Binding energy (BE) was calibrated to the C1s aliphatic component at 284.8 eV. Origin 2021 was used for visualizing spectra. Surface morphology was investigated on a selected piece of nanocomposite considered to be representative of the material. A Field emission- scanning electron microscope (FESEM) Zeiss Σigma 300 VP (Zeiss Oberkochen, Germany) equipped with an energy dispersive spectrometer (EDS) C-MaxN SDD (Oxford Instruments, Oxford, U.K.) with an active area of 20 $mm^2$ (Oxford Instruments, Oxford, U.K.) was used to perform analysis on the selected samples. The EDS spectrometer was calibrated using MAC standards (Micro-Analysis Consultants Ltd., United Kingdom) for elemental and mapping analysis.

TEM microscopy was performed with a FEI Tecnai 12 instrument (120 kV; filament $LaB_6$), by dropping catalyst suspensions on a carbon-coated Cu grid (300 mesh, TAAB). The catalyst was dispersed in isopropanol at 1 $gL^{-1}$.

### 2.4. Transesterification reaction

Catalytic tests were carried out in 10 mL glass vials equipped with a magnetic bar and sealed with a screw cap. The vial was charged with methanol (2 mL), soybean oil (350 μL, 322 mg), and 77 mg of composite Ca@CS.

The vial was then heated under stirring and left to react for the proper time. After the reaction time, the mixture was cooled to room temperature, transferred into a centrifuge tube, and subjected to 4000 rpm for 10 min.

After centrifugation, the methanolic phase (containing FAMEs and glycerol) was removed through a Pasteur pipette. Then the catalyst layer was washed with 4 mL of fresh methanol and centrifugated to eliminate traces of biodiesel and other organic residues. The operation described above is repeated twice. 100 μL of n-hexadecane was added to the combined methanolic phases as an internal standard, then the solution was evaporated to a small volume, and suspended in 10 mL of ethyl acetate. After drying, the ethyl acetate solution was subjected to qualitative and quantitative analyses by GC-MS to identify FAMEs and determine the composition of the biodiesel product.

### 2.5. Determination of FAMEs

FAMEs composition and yields were determined by GC–MS areas employing n-hexadecane as an internal standard. In the reacted solution, 100 μL (77 mg) of standard (hexadecane) were added and after workup, the final ethyl acetate solution was analyzed via GC–MS. The total mass of methyl esters ($m_{ME}$) was quantified by the following equation:

$$m_{ME} = \frac{A_{ME}}{A_S} \cdot f \cdot m_S \quad (1)$$

where $A_{ME}$ is the total GC–MS area of the peaks relevant to various fatty acid methyl ester products, $A_S$ is the area of the internal standard, f is the response factor of the instrument, and $m_S$ the added mass of the standard. More details are reported in the Supporting Information.

### 2.6. General procedure for recyclability tests of Ca@CS

The recyclability of the supported catalyst in the transesterification reaction of used soybean oil was carefully examined. After each run, the reaction tube was centrifugated and the liquid part was separated, leaving the catalyst in the vial. Then, fresh methanol was added (2 mL), and the operation described above was repeated twice to remove the FAMEs and to eliminate the organic residues, eventually present on the surface. The recovered catalyst was subsequently used for the next round of catalytic tests without further manipulation.

After the recyclability tests, Ca@CS was subjected to a "stress-test" to evaluate the features of an exhausted catalyst.

For this purpose, since the biodiesel yield was still high after 10 recycles (about 90 %, see Fig. 8), the catalyst was heated in methanol for 20 h at 120 °C, then recovered and used in a classical reaction, resulting in only a 10 % of conversion. The stressed Ca@CS was then subjected to several characterizations (SEM, ATR-FTIR, XPS) to investigate differences with the pristine material (See Section 3.3).

## 3. Results and discussion

### 3.1. Characterization of $Ca(OH)_2$ supported on chitosan

Ca@CS catalyst was characterized by ATR-FTIR before and after use, as shown in Fig. 1. The IR spectrum of chitosan alone is also presented for comparison.

The characteristic sharp peak at 3642 $cm^{-1}$, ascribed to O—H stretching in $Ca(OH)_2$, appears in both used and pristine catalysts, moreover partial carbonatation can be hypothesized since the band at about 1420 $cm^{-1}$ (carbonate antisymmetric stretching) and the peak at 872 $cm^{-1}$ (out-of-plane bending of $CO_3^{2-}$) are typical of $CaCO_3$ species. Signals relevant to the organic matrix are also readily visible, like N—H and O—H stretching modes in the 3200–3400 $cm^{-1}$ range, aliphatic C—H stretching below 3000 $cm^{-1}$, and CS characteristic bands between 1200 and 1000 $cm^{-1}$ corresponding to asymmetric stretching of the C—O—C bridge and C—O stretching. All assignments are in agreement with other works [59]. The catalyst usage does not seem to affect its chemical nature, even after several cycles, as demonstrated by the high similarity between IR spectra taken before and after the reaction.

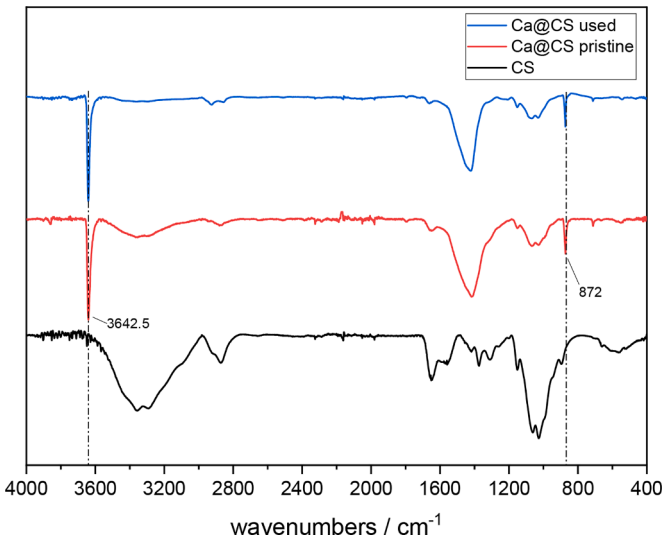


**Fig. 1.** ATR-FTIR spectra of the Ca@CS catalyst before (red curve) and after use (blue curve), black curve represents ATR-FTIR spectrum for chitosan.

The chemical surface composition of the catalyst and CS alone was investigated by XPS and the main elements were identified, as reported in Table 1. C, O, and N are mainly ascribed to chitosan, whereas Ca% indicates the successful integration of the inorganic component. Traces of other elements were found, but below 2 % total.

It can be noticed how Ca content remains almost constant even after ten cycling steps, thus suggesting that creating a hybrid-supported catalyst is a successful strategy for improving reusability and process yield. Moreover, the synthetic protocol adopted in this work seems to preserve the original organic matrix. In fact, the C1s region of pristine catalyst matches very well the typical appearance of the C1s region for chitosan [60], except for the last component at BE = 289.3 ± 0.3 eV attributed to $CaCO_3$ (Fig. S1a, Supporting Information). This finding is not surprising since the $Ca(OH)_2$ surface is mainly covered by $CaCO_3$ due to the carbonation process [61] (Fig. S1b, Supporting Information). Therefore, it was also found that $Ca2p_{3/2}$ position is compatible with $CaCO_3$ speciation [62] in consideration of the XPS sampling depth at the nanometer level. The used catalyst presents an increased carbon content and lower O/C and N/C ratios quite likely related to the partial adsorption of soybean oil on the support, as also corroborated by the C1s region showing a higher contribution of the aliphatic component at BE = 284.8 ± 0.2 eV (Fig. S1c, Supporting Information). On the other hand, the Ca2p spectrum appears almost identical to the one referred to pristine sample (Fig. S1d, Supporting Information), indicating that the catalyst overuse due to the transesterification reaction does not modify the calcium speciation.

As shown in Fig. 2, Ca@CS catalyst thermal behavior was analyzed by TGA and simultaneous DSC in the temperature range from 30 °C to 1000 °C under nitrogen flow. According to TGA, four weight losses were observed. The first one of 14.9 % at T lower than 100 °C can be ascribed to the loss of physiosorbed water from the hydrophilic structure of chitosan of the Ca@CS catalyst [63].

**Table 1**
Surface chemical composition (expressed in terms of element atomic%) as determined by XPS analysis. Error calculated on at least three sampling points.

| Sample | C% | O% | N% | Ca% | Cl% | Na% | F% |
|---|---|---|---|---|---|---|---|
| Ca@CS pristine | 42.6 ± 1.6 | 43.8 ± 1.0 | 2.4 ± 0.2 | 9.6 ± 0.7 | 0.4 ± 0.2 | 1.2 ± 0.3 | / |
| Ca@CS used | 51.0 ± 0.6 | 37.0 ± 0.5 | 2.0 ± 0.3 | 8.4 ± 0.5 | / | / | 1.6 ± 0.4 |
| CS | 59.6 ± 2.8 | 29.1 ± 0.5 | 5.2 ± 0.6 | / | 0.3 ± 0.2 | 5.8 ± 1.7 | / |

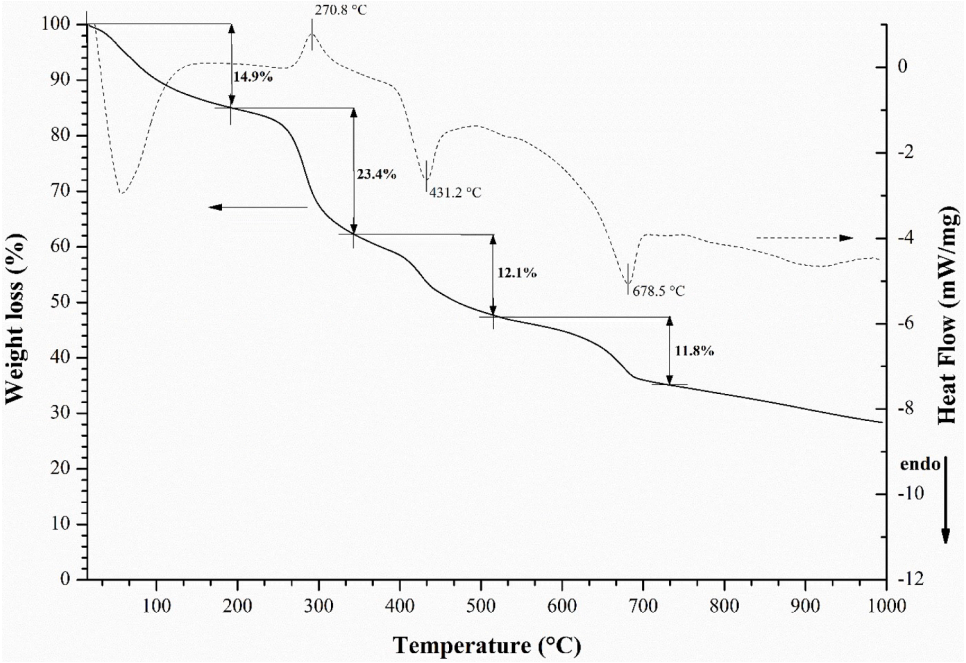


**Fig. 2.** TGA–DSC curves of the Ca@CS catalyst powders from 30 °C to 1000 °C.

At these temperatures ($T < 100$ °C) an endothermic peak associated with the dehydration process was observed. The second weight loss of 23.4 % corresponding to an exothermic peak centered at 270.8 °C can be assigned to the pyrolytic degradation of chitosan [63]. TGA of CS, acquired under nitrogen from 30 °C to 1000 °C and depicted in Figure S3, showed that after this first degradation process, CS underwent other pyrolytic processes of degradation until 1000 °C. The third weight loss step of 12.1 % corresponding to the endothermic peak at 431.2 °C was related to the decomposition of $Ca(OH)_2$ to CaO, while the fourth weight loss step of 11.8 % corresponding to the endothermic peak at 678.5 °C is ascribable to the decomposition of $CaCO_3$ to CaO [64]. The fourth peak showed the presence of $CaCO_3$ together with $Ca(OH)_2$ in the Ca@CS catalyst. Chitosan decomposition was responsible for the long tail in the TGA curve at high temperatures (750 °C–1000 °C) corresponding to the formation of a graphite-like structure of chitosan via dehydrogenation mechanism [65]. In Fig. 3, the TGA curve of the Ca@CS catalyst obtained carrying out the experiment in nitrogen flow below 800 °C and under air flow in the range from 800 °C to 1000 °C, is reported.

Considering the constant weight loss percentage above 800 °C corresponding to CaO residue after the chitosan combustion, the determined amount of calcium in the Ca@CS catalyst, expressed as CaO content, was ca. 27 %. Consequently, we can assume a content of Ca

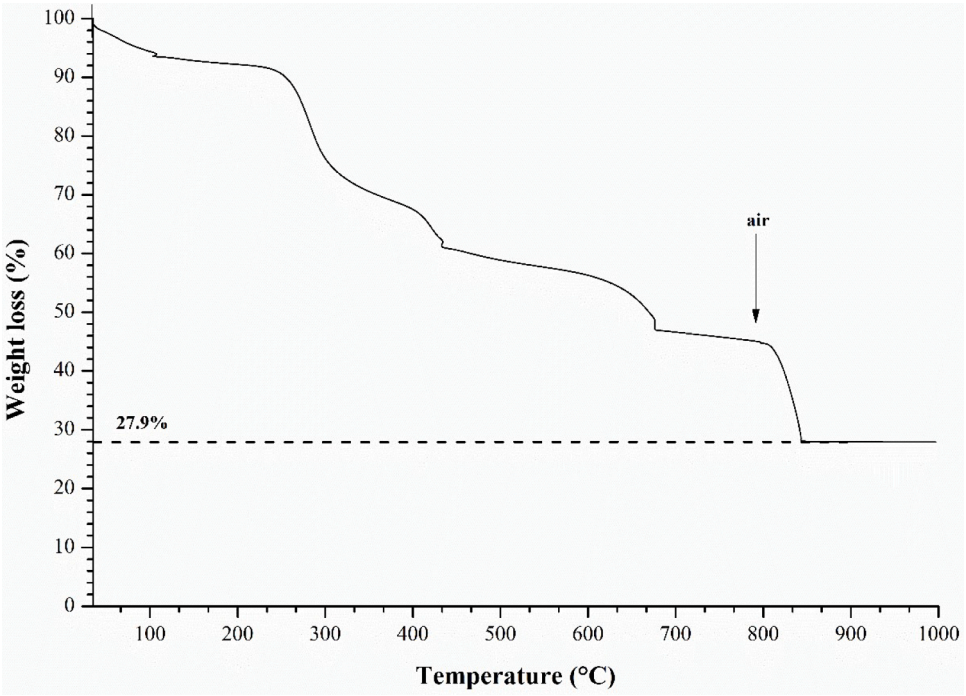


**Fig. 3.** TGA curve of the Ca@CS catalyst powders under nitrogen from 30 °C to 800 °C and in air flow from 800 °C to 1000 °C.

$(OH)_2$ in the composite equals to ca. 35.7 % in weight.

FESEM together with EDS analyses gave insight into the micro- and nano-scale features of the catalyst structure employing a morphological and chemical characterization. In Fig. 4 FESEM micrographs of CS alone and Ca@CS catalyst powders are reported (panels a, b). CS alone showed a compact and smooth macrostructure. This morphology changed after the alkaline precipitation of $Ca(OH)_2$ with the formation of the porous structure of the calcium hydroxide aggregates. Moreover, in the inset of the same panel, a TEM image shows that even at higher magnification inorganic particles compatible with calcium hydroxide lay on lower contrast flakes associated with chitosan.

SEM images acquired at higher magnifications (Fig. 4c-d) indicate that calcium hydroxide nanostructured aggregates present two kinds of morphology: a less abundant flower-like morphology composed of rod-like sub-units with lengths ranging between 170 nm and 700 nm (Fig. 4c) and a most diffuse hexagonal platelet stack morphology with sub-unit sizes which ranged from 160 nm to 2 μm (Fig. 4d). EDS mapping, performed using the carbon, nitrogen, and calcium elemental analyses, were applied to a selected area of a Ca@CS catalyst FESEM micrograph (Fig. 5) and revealed that hexagonal platelets were incorporated into the chitosan matrix.

### 3.2. Catalytic activity in biodiesel production

Different parameters relevant to the transesterification process on soybean oil were investigated to evaluate the performance of the proposed catalyst and the most appropriate conditions for its use, as demonstrated in the following paragraphs. Table 2 and Fig. 6 summarize the results of this study.

#### 3.2.1. Effects of the type of catalyst

The activity of the as-prepared Ca@CS catalyst in the transesterification reaction of commercial soybean oil with methanol was compared with unsupported calcium hydroxide catalysts having different particle sizes (Table 2).

At this end, both free calcium hydroxide submicrometric particles and bulk $Ca(OH)_2$ powder were used for comparison. As reported in Table 2, best results were obtained with Ca@CS composite and free Ca $(OH)_2$ submicrometric particles, indicating that the conversion into biodiesel is inversely related to particle size (entries 2–3).

This latter finding is in line with others reported in the literature under similar conditions [44,46] and seems to discredit the use of a supported catalyst since the yields are quite comparable. As reported later in the paper, and as might be expected, the robustness and ease of recycling of the proposed supported catalyst does justify its preparation and use. Note of mention, blank experiments carried out without catalyst and in the presence of the support alone, showed no catalytic activity (entries 4–5).

#### 3.2.2. Effect of catalyst loading

In this study, variable amounts of Ca@CS, ranging between 5 % to 30 % (catalyst/oil ratio, w/w), were used keeping methanol volume (4 mL) and oil mass (322 mg) constant. The reaction was carried out at 60 °C for 6 h.

In Fig. 6a, we observe the effect of catalyst amount on the resulting yield values. According to the graph, yield values reach a plateau once the catalyst loading surpasses 25 %. This peculiar behavior can be attributed to the quantity of suspended catalyst powder and the ratio of reaction volume, which can unpredictably influence the overall surface area. As a result, the number of active sites on the heterogeneous catalyst can be also impacted. [24].

#### 3.2.3. Effect of temperature

The role of temperature was considered in performing the reaction for 6 h and using 4 mL of methanol, 322 mg of oil, 77 mg of Ca@CS.

As shown in Fig. 6b, the catalyst is active even at temperatures just above room temperature (30–40 °C), providing satisfactory yields of 50–60 % in 6 h. However, a good compromise between reaction time and conversion was obtained at 60 °C, where the maximum yield of 100 % is reached within the same reaction time.

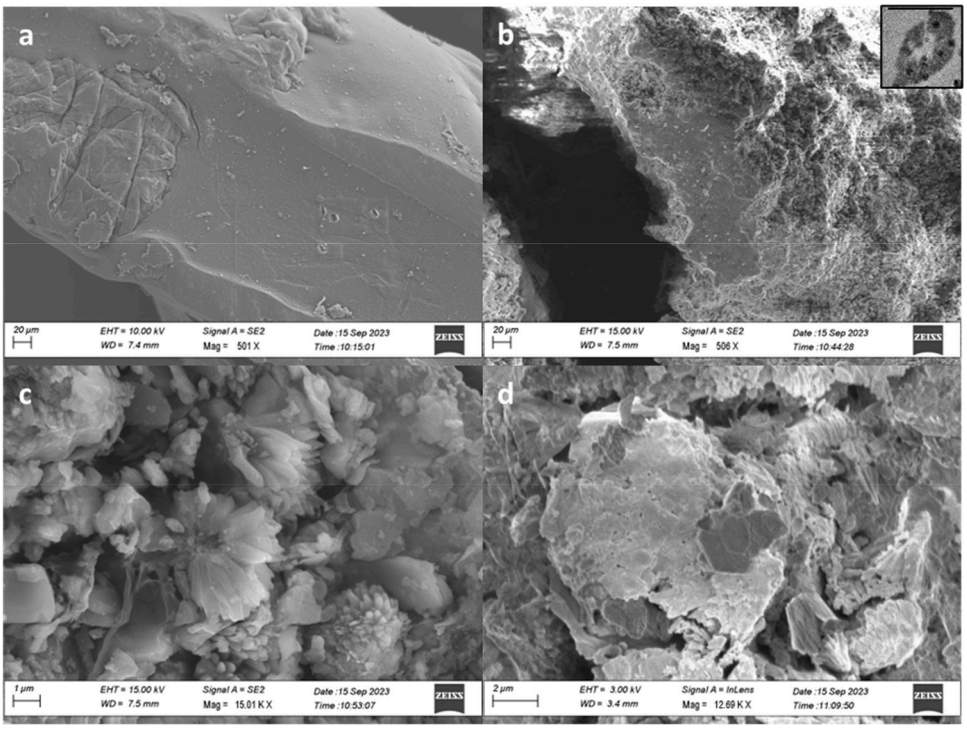


**Fig. 4.** FESEM images of CS (a) and Ca@CS catalyst (b-d) samples. A TEM image in the inset b shows a chitosan flake with nanometric structures on it (scale bar: 1 μm).

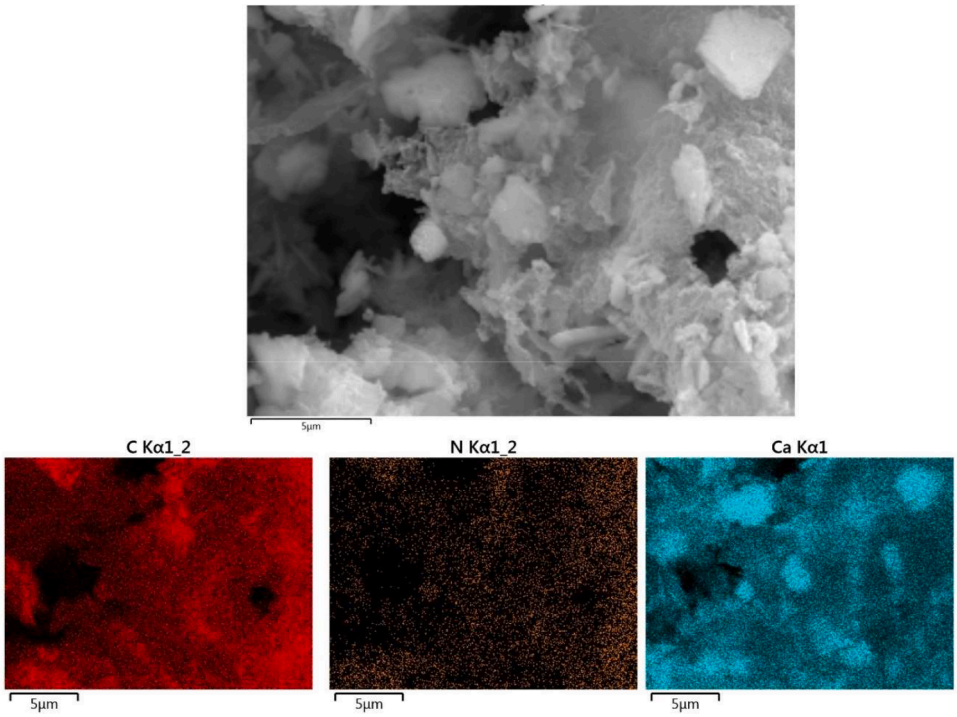


**Fig. 5.** FESEM image of Ca@CS catalyst sample and EDS mapping of carbon, nitrogen, and calcium elemental analyses.

**Table 2**
Transesterification reaction of soybean oil with methanol in the presence of Ca$(OH)_2$ based catalysts.

| Entry | Catalyst | FAMEs yield % |
|---|---|---|
| 1 | $Ca(OH)_{2\ bulk}$ | 61 |
| 2 | $Ca(OH)_2$ | 100 |
| 3 | Ca@CS | 98 |
| 4 | none | – |
| 5 | Chitosan | – |

*General conditions: soybean oil (350 µL, 322 mg), methanol (4 mL), catalyst (10 mg for entries 1–2, and 77 mg for entry 3), 60 °C, 6 h. Yields based on GC–MS data.

### 3.2.4. *Effect of methanol/oil ratio*

In this case, the methanol volume was varied using 322 mg of oil and 77 mg of Ca@CS. The reaction was carried out at 60 °C for 6 h.

An important parameter to set up in the transesterification reaction is the methanol/oil ratio. Stoichiometrically, 3 mol of alcohol are required to convert 1 mol of triglyceride. However, the methanol/oil ratio can be very different, depending on the reaction conditions, the nature of the catalyst and the type of oil.

Focusing on the use of $Ca(OH)_2$ as a catalyst, Sanchez-Cantù et al., using hydrated lime, succeeded in the transesterification of soybean oil with a $CH_3OH$/oil ratio of 0.17 (V/V) [46]. Later, the same authors employed a ratio of 0.42 (V/V), using castor oil [44], and 0.51 (V/V), with the same oil, but with calcium diglyceroxide as the catalyst [66].

In 2012, Chen et al. studied the use of calcium hydroxide obtained from the hydrolysis of calcium carbide. In this case, with used soybean oil, they found 0.54 (12:1 methanol/oil molar ratio) as the best proportion [45].

More recently, Promarak et al., with palm oil and hydrated lime-derived CaO as heterogeneous catalyst, found an optimal ratio equal to 1.25 to reach a complete conversion [41].

In principle, a large amount of methanol can drive the reaction in favor of the products, but some drawbacks have to be considered, such as the rise of the costs, due to the alcohol recovery. However, under heterogeneous conditions, a methanol excess can be advantageous, since glycerol is dissolved in methanol, thus facilitating the removal of by-products from the surface of the catalyst, which is promptly available for recycling [51].

Accordingly, we recently found a best ratio of 12:1 (V/V) in the (trans)esterification of soybean oil and free fatty acids with methanol when using steel slags [22] or clays [21], confirming the need for an excess of alcohol. As shown in Fig. 6c, this ratio can dramatically affect the reaction outcome, and an increase from a 4:1 (V/V) to a 6:1 (V/V) was sufficient to raise the conversion from 60 % to completion.

### 3.2.5. *Effect of reaction time*

Considering the best methanol/oil volume ratio estimated for this catalyst, 322 mg of oil and 2 mL of methanol were reacted in the presence of 77 mg Ca@CS at 60 °C for different times.

The optimal reaction time was evaluated by studying the reaction in a range from 1 h to 6 h, at 60 °C. As displayed in Fig. 6d, the conversion increased with time, reaching a maximum yield at 6 h.

For shorter reaction times, a sort of induction period seems to be present, since biodiesel yield rapidly rises from 20 % (2 h) to 80 % (3 h) in only 1 h.

This may be typical under heterogeneous conditions due to a change in the composition of the active catalyst (reasonably, the formation of a coordinated methoxide ion and a protonated catalyst), and/or to the initial adsorption of reagents on the composite surface (for the reaction mechanism, *vide infra*).

### 3.2.6. *Kinetic insight*

To evaluate the Ca@CS catalyst activity, activation energy ($E_a$) was calculated and compared with that of analogous Ca-based materials. In the presence of an excess of methanol it is possible to assume that the transesterification of triglycerides is a pseudo-first order reaction [67]. The rate of transesterification can be expressed by Eq. (2):

$$r = -\frac{d[TG]}{dt} = k'\cdot[TG]\cdot[ROH]^3 \quad (2)$$

Accordingly, the rate equation can be expressed as:

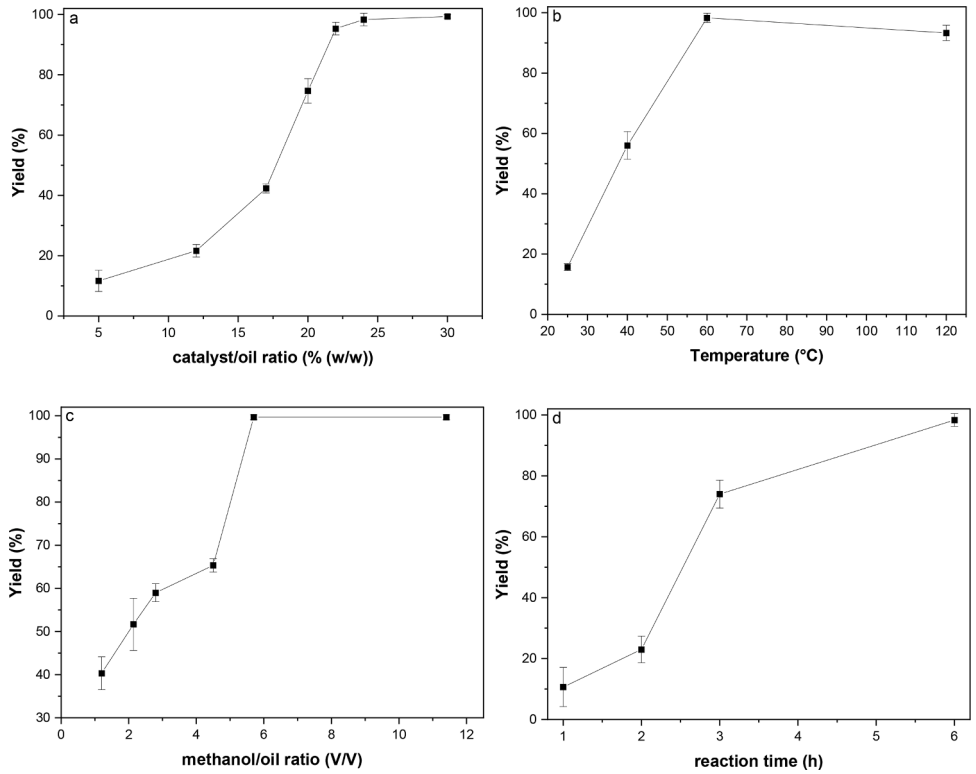


**Fig. 6.** Effect of different parameters on the transesterification process using Ca@CS catalyst: a) catalyst/oil ratio, b) reaction temperature, c) methanol/oil ratio, d) reaction time.

$$r = -\frac{d[TG]}{dt} = k\cdot[TG] \quad (3)$$

where $k = k'\cdot[ROH]^3$. In addition:

$$r = -\frac{dX_r}{dt} = k\cdot(1 - X_r) \quad (4)$$

where $X_r$ is the TG conversion into FAMEs ($X_r = 1 - [TG]/[TG]_0$) and the integrated equation is:

$$-\ln(1 - X_r) = k\cdot t \quad (5)$$

The plot of -ln (1-$X_r$) against $t$ was used to determine the rate constant $k$ (as the slope). Experiments were carried out in the range of

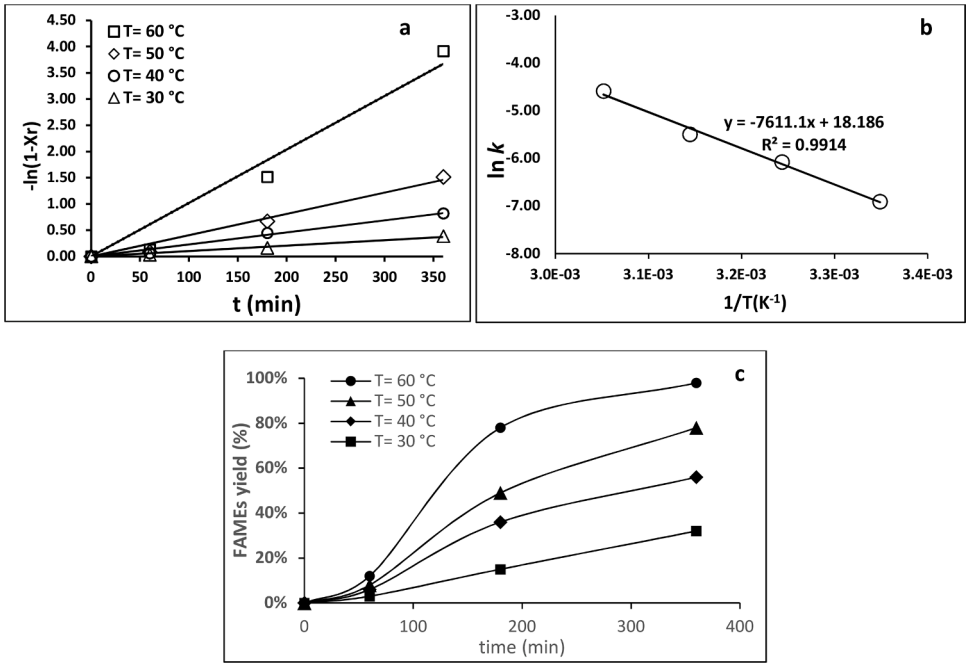


**Fig. 7.** (a) Plot of -ln(1-$X_r$) versus reaction time at the studied temperatures; (b) Arrhenius plot of ln $k$ vs 1/T for kinetic parameter $E_a$ evaluation; (c) Plot of yields as a function of time at different temperatures.

temperatures of 30 – 60 °C (Fig. 7a) [41].

Rate constant values ($k$) were found in a similar range as compared to the values reported in the literature [24] and were used to calculate activation energy ($E_a$) through Arrhenius equation (Eq. (6)) and from the slope of the linear correlation resulting of plotting ln $k$ versus 1/T (Eq. (7) and Fig. 7b).

$$k = A \cdot e^{-E_a/RT} \tag{6}$$

$$ln\ k = ln\ A - \frac{E_a}{RT} \tag{7}$$

The calculated $E_a$ value of 63.25 kJ·mol$^{-1}$ is in agreement with data reported in the literature, which usually reports for transesterification of triglycerides an activation energy value ranging in the range 50 – 120 kJ·mol$^{-1}$ [41,44,46,66]. From these data it clearly emerged that Ca@CS catalyst displays a kinetic behavior quite similar to that of most of the analogous Ca-based heterogenous catalytic systems, but without requiring tedious and costly preparations (e.g., calcination, nano-structuration etc.) and showing simultaneously a superior resistance to recycling procedures (see Section 3.3).

### 3.3. Catalyst recycle

The catalyst robustness was evaluated through appropriate recycling experiments. This is a crucial point in heterogeneous catalysis since the feasibility and economic sustainability of the entire process depend on the possibility of reusing the catalyst. After each run, reaction mixture was centrifuged and supernatant methanolic solution (containing FAMEs and glycerol) was recovered, while catalyst powder was washed twice with fresh methanol to remove organic residues.

The recovered composite was subsequently used for the next round of catalytic tests without further manipulations, by adding fresh amounts of oil and methanol, while the combined methanolic solutions were treated for FAMEs quantification (see Section 2.5 for details).

Data reported in Fig. 8 show the catalyst's surprising robustness, as many recycles were possible: at the tenth reuse, the composite still shows a 90 percent yield. This is the best result among those obtained with calcium hydroxide and is comparable to, if not better, than other oxide-based catalysts.

Fluctuations in yields among runs can be considered typical of a heterogeneous system in which, unlike in a homogeneous one, factors such as heat and mass transfers between phases, particularly with highly indented materials, can have an important impact on the final result of the reaction [68]. In addition, small variations in surface catalyst particle size or geometry between recycles can lead to a pattern of results such as that shown in Fig. 8.

Furthermore, as stated by other authors, a change in the catalyst nature can also occur after the first reuse, leading to a drop in biodiesel conversion after a few cycles, and then to a rise, after the catalyst modification [44].

To evaluate if $Ca(OH)_2$ was altered in size and/or geometry or, on the contrary, completely or in part replaced by calcite and/or calcium diglyceroxide, SEM-EDS, XPS, ATR-FTIR characterizations were performed on the catalyst after the tenth recycle. In order to enhance the differences, a comparison was also made with the catalyst previously subjected to a specific stress test (See Section 2.5).

In the FESEM image of the low active Ca@CS (Fig. 9b) calcium hydroxide structures are noticeably reduced and observed outside the chitosan support microparticles in comparison with a used active Ca@CS (Fig. 9a). As observed in the FESEM image of the not active Ca@CS catalyst sample (Fig. 9b'), $Ca(OH)_2$ particles loose the defined hexagonal shape (Fig. 9a') assuming a quasi-rhombohedral form. Moreover, EDS analysis performed on the selected area of the FESEM micrographs revealed a decrease in the calcium content of the non-

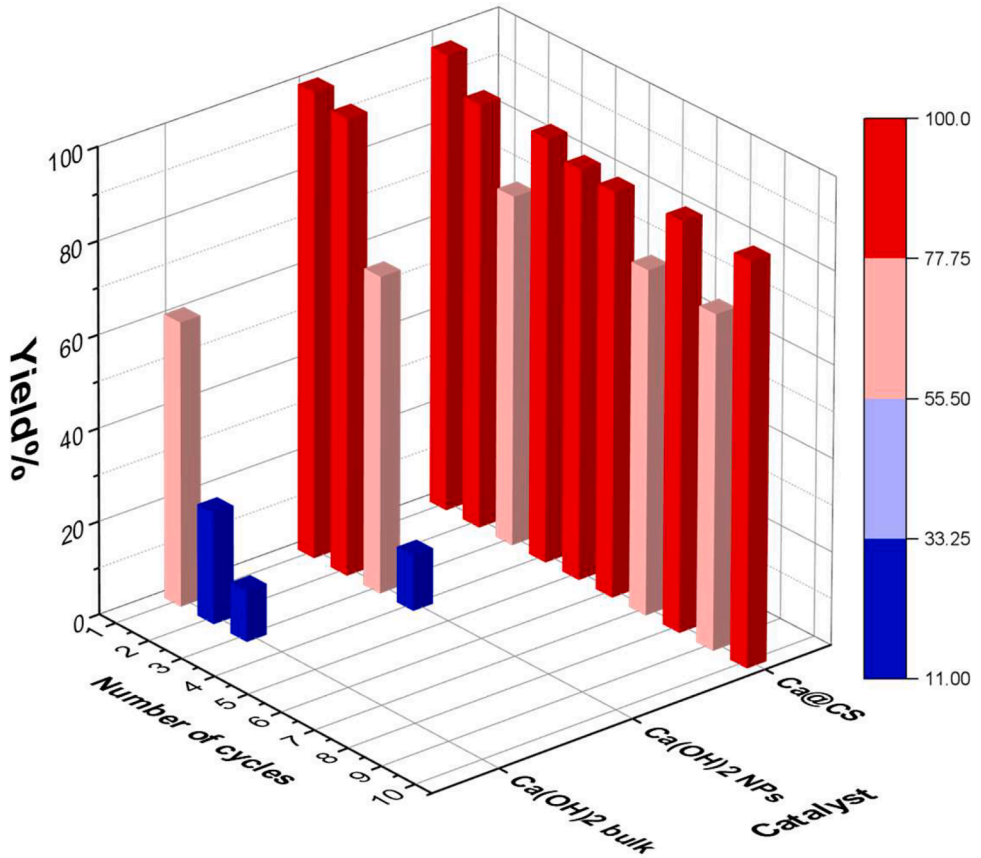


**Fig. 8.** Comparison among commercial $Ca(OH)_2$, unsupported submicrometric particles ($Ca(OH)_2$ NPs), and Ca@CS catalysts in recyclability tests.

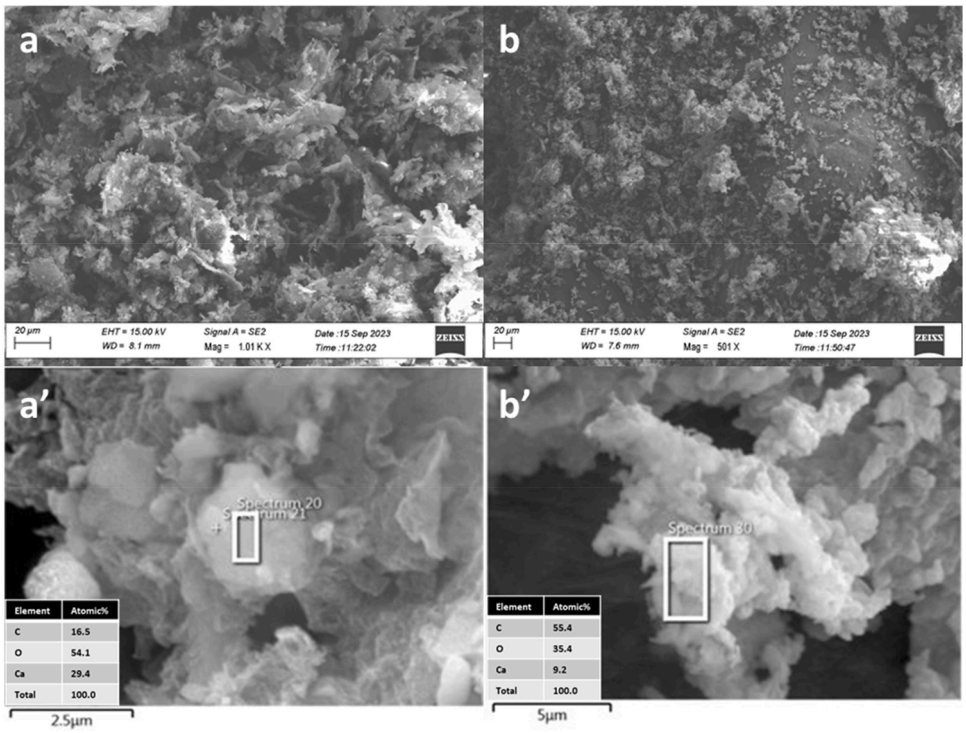


**Fig. 9.** FESEM images of a-a') used active and b-b') exhausted Ca@CS catalyst samples. Corresponding EDS analyses are also reported.

active Ca@CS catalyst sample with respect to the active Ca@CS.

Spectroscopic characterization of exhausted catalyst corroborated SEM-EDS results. Fig. S2 shows ATR-FTIR spectrum (panel a) and C1s (panel b), Ca2p (panel c) XP spectra of the inactive Ca@CS sample. IR spectrum indicates unequivocally that calcium hydroxide is absent (disappearance of signal at 3642 $cm^{-1}$) and only $CaCO_3$ is still present, moreover main signals can be associated to the adsorption of FAME (diagnostic signal at 1743 $cm^{-1}$) on the catalyst surface. Similarly, C1s region (Fig. S2b, Supporting Information) confirms that such adsorption occurred. $Ca2p_{3/2}$ position (Fig. S2c, Supporting Information) is also slightly shifted at 347.3 eV, which is assigned to $CaCO_3$. Finally, XPS quantitative analysis demonstrated a significant reduction of Ca% content below 1.5 %.

On the contrary, it seems that the used catalyst does not undergo any evident alterations when compared with the pristine catalyst, as evidenced by FESEM pictures and EDS analyses (Fig. 9, images a-a'), which suggest that there was no change in the catalytic nature even after several cycles.

### 3.4. Multigram scale reaction

To validate this method, we also performed a multigram scale experiment. For this purpose, waste cooking oil (WCO) was employed, as waste oils are considered a promising alternative in biodiesel synthesis due to their low cost and high availability [69]. From a circular economy perspective, waste oils are two to three times cheaper than refined vegetable oils because they represent a waste, without the costs of removal and treatment [70]. In addition, the use of WCO can help to reduce competition with food demand.

The chemical composition of WCO is reported in the Supporting Information [21].

To this end, 3.15 mL of filtered oil was treated with 36 mL of methanol and 693 mg of catalyst, at 60 °C. We were favourably surprised to find that the reaction occurred to completion even on a larger scale and with waste oil. In fact, after 6 h, the WCO produced biodiesel with a chromatographic yield of 100 % and an isolated yield of 84 %, demonstrating the feasibility of the proposed protocol.

### 3.5. Hot filtration test and mechanistic insights

Some researchers have proposed possible mechanisms for solid-based catalysts [26,44,46].

To assess the degree of heterogeneity of the whole process, hot filtration tests were carried out, and the results are shown in Fig. 10.

Data in Fig. 10 clearly show that catalytic activity dropped down when the Ca@CS composite was removed from the reaction mixture (see dashed lines in Fig. 10), thus confirming that catalysis is heterogeneous in nature and that the metal leaching or the presence of alkoxide anions (methoxide or diglyceroxide) dissolved in the solution can be neglected.

The available data suggests that the catalytic reaction occurs on the surface of calcium hydroxide. In line with the transesterification

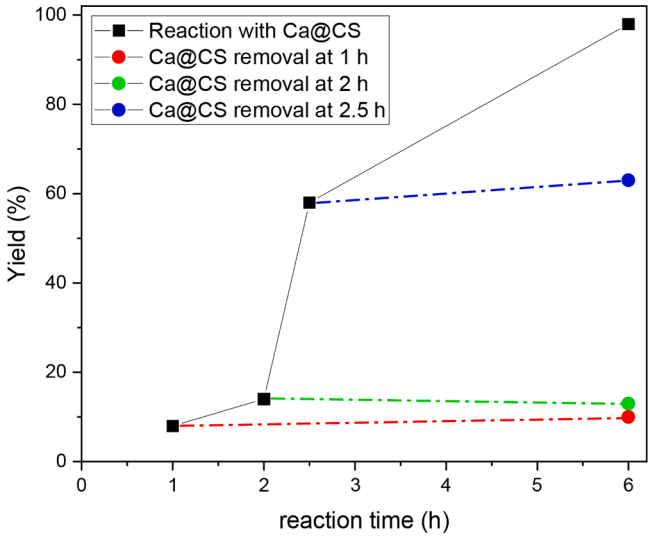


**Fig. 10.** Hot filtration test conducted at different reaction times.

mechanism of triglycerides reported in the literature for a heterogeneous catalyst based on $Ca(OH)_2$, [44] it can be hypothesized that when methanol and triglyceride molecules encounter adjacent catalytic sites ($OH^-$ and $Ca^{2+}$), they react with them: the $OH^-$ site present on the surface removes an $H^+$ from the methanol molecule, while the $Ca^{2+}$ site absorbs $CH_3O^-$. Additionally, chitosan can adsorb triglycerides by creating a layer on the surface (*vide infra*). This layer helps in the interaction of the two neighboring species, leading to the generation of fatty acid methyl esters and diglycerides. The diglyceride, upon reacting with methanol in a similar process on the catalyst surface, creates glycerol and biodiesel [44].

### 3.5.1. Role of the chitosan support

Comparison with other sources of $Ca(OH)_2$ (Fig. 8) clearly shows the importance of chitosan support for the robustness and recyclability of the composite and of particle size for catalyst activity. In fact, bulk calcium hydroxide is poorly active in the transesterification reaction, and its performance decays dramatically after the first use. Similarly, free $Ca(OH)_2$ nanoparticles are very active, but undergo a rapid loss of activity after two cycles.

Chitosan, which is a poly-cationic biopolymer, can act as an emulsifier and emulsion stabilizer and can interact directly with soybean oil triacylglycerides without the need for additional surfactants. As a consequence, because of chitosan's ability to bind free fatty acids or triglycerides, the reactants are closer to the catalytic sites and can react more easily (Fig. 11) [71,72].

Furthermore, the capacity of chitosan to bind cations such as calcium, more than cellulose, is well known and metal ion chelation is employed, for example, in drug delivery or in the removal of metal pollutants from wastewater [73].

This feature can be very important in trapping any free calcium ions in the leached solution during the reaction, which has several important effects: prolonging catalyst life, preventing soap formation in the presence of free fatty acids, and avoiding the release of calcium cations into the final biodiesel.

## 4. Conclusions

In conclusion, we presented here the facile synthesis of a catalyst based on calcium hydroxide nanoparticles supported on chitosan. This composite is the first example of calcium hydroxide nanoparticles supported on chitosan used in biodiesel synthesis. The catalyst has been fully characterized and has been used in the synthesis of FAMEs from soybean oil and methanol. The most important parameters in the transesterification reaction have been investigated, and a methanol/oil ratio of 6:1, 6 h reaction, and 60 °C allow for complete conversion. The reaction was also tested on the gram scale with excellent results, by using waste oil as starting material. In addition, the catalyst proved to be robust, as after the 10th recycle, the conversion was still around 90 %, without any apparent leaching of active species. As proof, SEM-EDS, XPS, ATR-FTIR analyses on the recycled catalyst, showed a constant Ca content, even after ten cycles, thus suggesting that creating a hybrid-supported catalyst is a successful strategy for improving reusability and process yield. In comparison, a "stressed" and inactive catalyst, shows reduced calcium hydroxide structures located outside the chitosan support microparticles. Moreover, even the geometry is different, since $Ca(OH)_2$ particles lose the defined hexagonal shape assuming a quasi-rhombohedral form.

The activation energy ($E_a$) was calculated and compared with that of analogous Ca-based materials. An Ea value of 63.25 $kJ \cdot mol^{-1}$ was found, which is in agreement with data reported in the literature. Finally, some evidence on the heterogeneous nature of the catalysis was provided with the help of the hot filtration test. In addition, it was evaluated that chitosan, as a support, has the potential to act as an emulsifier and emulsion stabilizer. It can interact directly with soybean oil triacylglycerides without requiring additional surfactants. As a result, chitosan can bind free fatty acids or triglycerides, which brings the reactants closer to the catalytic sites, making it easier for them to react. Studies are still ongoing to verify the scalability of the proposed protocol. Moreover, research will prosecute checking the quality of the produced biodiesel according to international standards.

## CRediT authorship contribution statement

**A. Aloia:** Investigation, Data curation. **M. Izzi:** Investigation, Data curation. **A. Rizzuti:** Investigation, Data curation. **M. Casiello:** Investigation. **P. Mastrorilli:** Supervision, Data curation. **N. Cioffi:** Supervision. **A. Nacci:** Writing – original draft, Validation, Supervision, Data curation. **R.A. Picca:** Writing – review & editing, Writing – original draft, Validation, Investigation, Data curation. **A. Monopoli:** Writing – review & editing, Writing – original draft, Validation, Supervision, Methodology, Data curation, Conceptualization.

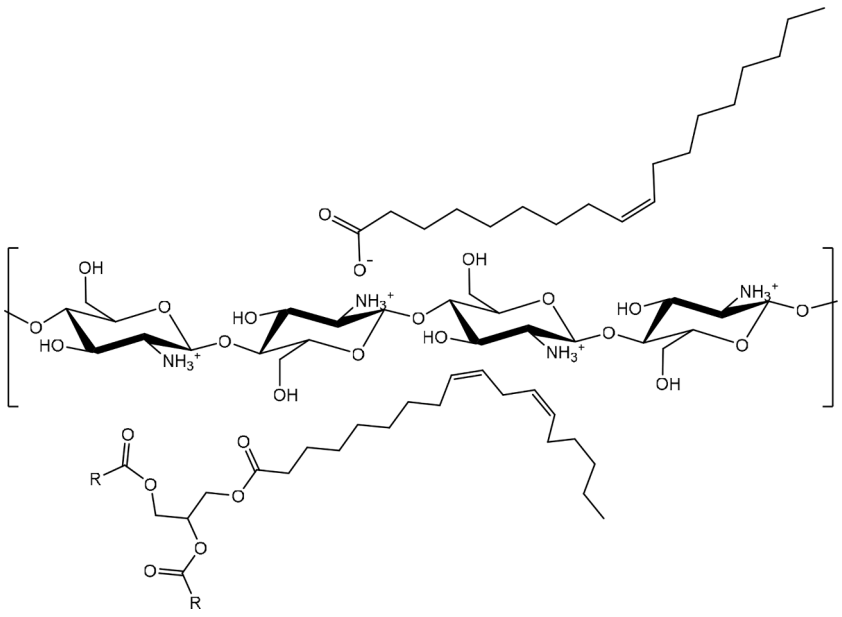


**Fig. 11.** Chitosan acting as an emulsifier toward triglycerides and free fatty acids.

## Declaration of competing interest

The authors declare that they have no known competing financial interests or personal relationships that could have appeared to influence the work reported in this paper.

## Data availability

Data will be made available on request.

## Acknowledgments

The authors thanks Mr. D. Calia for partial support in the experimental work. "This research was partially funded by the European Union-19 FESR "PON Ricerca e Innovazione 2014–2020. Progetto: 20 Energie per l'Ambiente TARANTO-Cod. ARS01_00637" and by "Research for Innovation (REFIN)" – POR Puglia FESR FSE 2014-2020, Project ID 4A20B1C8.

## Supplementary materials

Supplementary material associated with this article can be found, in the online version, at doi:10.1016/j.mcat.2024.114128.

## References

[1] D.-G. for C. European Commission, Tackling rising energy prices: a toolbox for action and support, Publ. Off. Eur. Union. (2021). https://data.europa.eu/doi/10.2775/99874.
[2] Renewable energy, Fact Sheets Eur. Union. (2023) 1–7. www.europarl.europa.eu/factsheets/en.
[3] European Commission, The European Green Deal, Eur. Comm. 53 (2019) 24, https://doi.org/10.1017/CBO9781107415324.004.
[4] A.G. Alsultan, N. Asikin Mijan, N. Mansir, S.Z. Razali, R. Yunus, Y.H. Taufiq-Yap, Combustion and emission performance of CO/NO x /SO x for green diesel blends in a swirl burner, ACS Omega 6 (2021) 408–415, https://doi.org/10.1021/acsomega.0c04800.
[5] L. Leng, W. Li, H. Li, S. Jiang, W. Zhou, Cold flow properties of biodiesel and the improvement methods: a review, Energy Fuels 34 (2020) 10364–10383, https://doi.org/10.1021/acs.energyfuels.0c01912.
[6] I. Shahid, A. Siddique, T. Nawaz, M.B. Tahir, J. Fatima, A. Hussain, J. ur Rehman, M.A. Assiri, M. Imran, M. Alzaid, H. Alrobei, Heterogeneous nanocatalyst for biodiesel fuel production: bench scale from waste oil sources, Zeitschrift Für Phys. Chemie 236 (2022) 1377–1410, https://doi.org/10.1515/zpch-2021-3160.
[7] K. Ngaosuwan, A. Eiad-ua, A. Srifa, W. Kiatkittipong, W. Appamana, D. Wongsawaeng, A.T. Quitain, S. Assabumrungrat, Application of catalysts derived from renewable resources in production of biodiesel. Biodiesel Prod, Wiley, 2022, pp. 229–248, https://doi.org/10.1002/9781119771364.ch12.
[8] S. Chandra Kishore, S. Perumal, R. Atchudan, A.K. Sundramoorthy, M. Alagan, S. Sangaraju, Y.R. Lee, A review of biomass-derived heterogeneous catalysts for biodiesel production, Catalysts 12 (2022) 1501, https://doi.org/10.3390/catal12121501.
[9] A. Marwaha, A. Dhir, S.K. Mahla, S.K. Mohapatra, An overview of solid base heterogeneous catalysts for biodiesel production, Catal. Rev. 60 (2018) 594–628, https://doi.org/10.1080/01614940.2018.1494782.
[10] S. Semwal, A.K. Arora, R.P. Badoni, D.K. Tuli, Biodiesel production using heterogeneous catalysts, Bioresour. Technol. 102 (2011) 2151–2161, https://doi.org/10.1016/j.biortech.2010.10.080.
[11] A.P.S. Chouhan, A.K. Sarma, Modern heterogeneous catalysts for biodiesel production: a comprehensive review, Renew. Sustain. Energy Rev. 15 (2011) 4378–4399, https://doi.org/10.1016/j.rser.2011.07.112.
[12] C. Carlucci, L. Degennaro, R. Luisi, Titanium dioxide as a catalyst in biodiesel production, Catalysts 9 (2019) 75, https://doi.org/10.3390/catal9010075.
[13] J. Zhu, W. Jiang, Z. Yuan, J. Lu, J. Ding, Esterification of tall oil fatty acid catalyzed by Zr4+-CER in fixed bed membrane reactor, Renew. Energy 221 (2024) 119760, https://doi.org/10.1016/j.renene.2023.119760.
[14] M. Guo, W. Jiang, J. Ding, J. Lu, Highly active and recyclable CuO/ZnO as photocatalyst for transesterification of waste cooking oil to biodiesel and the kinetics, Fuel 315 (2022) 123254, https://doi.org/10.1016/j.fuel.2022.123254.
[15] A. Wang, W. Quan, H. Zhang, H. Li, S. Yang, Heterogeneous ZnO-containing catalysts for efficient biodiesel production, RSC Adv. 11 (2021) 20465–20478, https://doi.org/10.1039/D1RA03158A.
[16] P.M. Varol, A. Çakan, B. Kiren, N. Ayas, Microwave-assisted catalytic transesterification of soybean oil using KOH/γ-Al2O3, Biomass Convers. Biorefinery 13 (2023) 633–645, https://doi.org/10.1007/s13399-020-01253-4.
[17] I. Yaqoob, U. Rashid, F. Nadeem, Alumina supported catalytic materials for biodiesel production - a detailed review, Int. J. Chem. Biochem. Sci. 16 (2019) 41–53.
[18] J.P. da Costa Evangelista, A.D. Gondim, L. Di Souza, A.S. Araujo, Alumina-supported potassium compounds as heterogeneous catalysts for biodiesel production: a review, Renew. Sustain. Energy Rev. 59 (2016) 887–894, https://doi.org/10.1016/j.rser.2016.01.061.
[19] S. Mardiana, N.J. Azhari, T. Ilmi, G.T.M. Kadja, Hierarchical zeolite for biomass conversion to biofuel: a review, Fuel 309 (2022) 122119, https://doi.org/10.1016/j.fuel.2021.122119.
[20] M. Shahinuzzaman, Z. Yaakob, Y. Ahmed, Non-sulphide zeolite catalyst for bio-jet-fuel conversion, Renew. Sustain. Energy Rev. 77 (2017) 1375–1384, https://doi.org/10.1016/j.rser.2017.01.162.
[21] M. Casiello, S. Savino, M. Massaro, L.F. Liotta, G. Nicotra, C. Pastore, C. Fusco, A. Monopoli, L. D'Accolti, A. Nacci, S. Riela, Multifunctional halloysite and hectorite catalysts for effective transformation of biomass to biodiesel, Appl. Clay Sci. 242 (2023) 107048, https://doi.org/10.1016/j.clay.2023.107048.
[22] M. Casiello, O. Losito, A. Aloia, D. Caputo, C. Fusco, R. Attrotto, A. Monopoli, A. Nacci, L. D'Accolti, Steel slag as new catalyst for the synthesis of fames from soybean oil, Catalysts 11 (2021) 619, https://doi.org/10.3390/catal11050619.
[23] M. Massaro, M. Casiello, L. D'Accolti, G. Lazzara, A. Nacci, G. Nicotra, R. Noto, A. Pettignano, C. Spinella, S. Riela, One-pot synthesis of ZnO nanoparticles supported on halloysite nanotubes for catalytic applications, Appl. Clay Sci. 189 (2020) 105527, https://doi.org/10.1016/j.clay.2020.105527.
[24] M. Casiello, L. Catucci, F. Fracassi, C. Fusco, A. Laurenza, L. di Bitonto, C. Pastore, L. D'Accolti, A. Nacci, ZnO/Ionic liquid catalyzed biodiesel production from renewable and waste lipids as feedstocks, Catalysts 9 (2019) 71, https://doi.org/10.3390/catal9010071.
[25] B. Notarnicola, G. Tassielli, P.A. Renzulli, R. Di Capua, F. Astuto, S. Riela, A. Nacci, M. Casiello, M.L. Testa, L.F. Liotta, C. Pastore, Life Cycle Assessment of a system for the extraction and transformation of Waste Water Treatment Sludge (WWTS)-derived lipids into biodiesel, Sci. Total Environ. 883 (2023) 163637, https://doi.org/10.1016/j.scitotenv.2023.163637.
[26] D.M. Marinković, M.V. Stanković, A.V. Veličković, J.M. Avramović, M. R. Miladinović, O.O. Stamenković, V.B. Veljković, D.M. Jovanović, Calcium oxide as a promising heterogeneous catalyst for biodiesel production: current state and perspectives, Renew. Sustain. Energy Rev. 56 (2016) 1387–1408, https://doi.org/10.1016/j.rser.2015.12.007.
[27] N. Widiarti, H. Bahruji, H. Holilah, Y.L. Ni'mah, R. Ediati, E. Santoso, A.A. Jalil, A. Hamid, D. Prasetyoko, Upgrading catalytic activity of NiO/CaO/MgO from natural limestone as catalysts for transesterification of coconut oil to biodiesel, Biomass Convers. Biorefinery 13 (2023) 3001–3015, https://doi.org/10.1007/s13399-021-01373-5.
[28] H. Mazaheri, H.C. Ong, Z. Amini, H.H. Masjuki, M. Mofijur, C.H. Su, I. Anjum Badruddin, T.M.Y. Khan, An overview of biodiesel production via calcium oxide based catalysts: current state and perspective, Energies 14 (2021) 3950, https://doi.org/10.3390/en14133950.
[29] M.G. Weldeslase, N.E. Benti, M.A. Desta, Y.S. Mekonnen, Maximizing biodiesel production from waste cooking oil with lime-based zinc-doped CaO using response surface methodology, Sci. Rep. 13 (2023) 4430, https://doi.org/10.1038/s41598-023-30961-w.
[30] A.P. Soares Dias, J. Puna, J. Gomes, M.J. Neiva Correia, J. Bordado, Biodiesel production over lime. Catalytic contributions of bulk phases and surface Ca species formed during reaction, Renew. Energy 99 (2016) 622–630, https://doi.org/10.1016/j.renene.2016.07.033.
[31] M.-C. Hsiao, J.-Y. Kuo, S.-A. Hsieh, P.-H. Hsieh, S.-S. Hou, Optimized conversion of waste cooking oil to biodiesel using modified calcium oxide as catalyst via a microwave heating system, Fuel 266 (2020) 117114, https://doi.org/10.1016/j.fuel.2020.117114.
[32] M.E. Bambase, R.A.R. Almazan, R.B. Demafelis, M.J. Sobremisana, L.S.H. Dizon, Biodiesel production from refined coconut oil using hydroxide-impregnated calcium oxide by cosolvent method, Renew. Energy 163 (2021) 571–578, https://doi.org/10.1016/j.renene.2020.08.115.
[33] W. Widayat, T. Darmawan, H. Hadiyanto, R.A. Rosyid, Preparation of heterogeneous CaO catalysts for biodiesel production, J. Phys. Conf. Ser. 877 (2017) 8–15, https://doi.org/10.1088/1742-6596/877/1/012018.
[34] C.V.R. Moura, W.C. Abreu, E.M. Moura, J.C.S. Costa, CaO derived from waste shell materials as catalysts in synthesis of biodiesel. Waste and Biodiesel, Elsevier, 2022, pp. 91–118, https://doi.org/10.1016/B978-0-12-823958-2.00001-X.
[35] F. Yaşar, Biodiesel production via waste eggshell as a low-cost heterogeneous catalyst: its effects on some critical fuel properties and comparison with CaO, Fuel 255 (2019) 115828, https://doi.org/10.1016/j.fuel.2019.115828.
[36] N.A. Ali, N. Khairuddin, B.M. Siddique, Eggshell waste as a catalyst for biodiesel production: a preliminary study, IOP Conf. Ser. Mater. Sci. Eng. 1195 (2021) 012043, https://doi.org/10.1088/1757-899x/1195/1/012043.
[37] E. Fayyazi, B. Ghobadian, H.H. van de Bovenkamp, G. Najafi, B. Hosseinzadehsamani, H.J. Heeres, J. Yue, Optimization of biodiesel production over chicken eggshell-derived CaO catalyst in a continuous centrifugal contactor separator, Ind. Eng. Chem. Res. 57 (2018) 12742–12755, https://doi.org/10.1021/acs.iecr.8b02678.
[38] I. Gaide, V. Makareviciene, E. Sendzikiene, Effectiveness of eggshells as natural heterogeneous catalysts for transesterification of rapeseed oil with methanol, Catalysts 12 (2022) 246, https://doi.org/10.3390/catal12030246.
[39] Z. Wei, C. Xu, B. Li, Application of waste eggshell as low-cost solid catalyst for biodiesel production, Bioresour. Technol. 100 (2009) 2883–2885, https://doi.org/10.1016/j.biortech.2008.12.039.

[40] W. Liu, N.W. Low, B. Feng, G. Wang, J.C. Diniz da Costa, Calcium precursors for the production of CaO sorbents for multicycle CO2 capture, Environ. Sci. Technol. 44 (2010) 841–847, https://doi.org/10.1021/es902426n.
[41] W. Roschat, T. Siritanon, B. Yoosuk, V. Promarak, Biodiesel production from palm oil using hydrated lime-derived CaO as a low-cost basic heterogeneous catalyst, Energy Convers. Manag. 108 (2016) 459–467, https://doi.org/10.1016/j.enconman.2015.11.036.
[42] M.L. Granados, M.D.Z. Poves, D.M. Alonso, R. Mariscal, F.C. Galisteo, R. Moreno-Tost, J. Santamaría, J.L.G. Fierro, Biodiesel from sunflower oil by using activated calcium oxide, Appl. Catal. B Environ. 73 (2007) 317–326, https://doi.org/10.1016/j.apcatb.2006.12.017.
[43] C. Chen, S. Qu, M. Guo, J. Lu, W. Yi, R. Liu, J. Ding, Waste limescale derived recyclable catalyst and soybean dregs oil for biodiesel production: analysis and optimization, Process Saf. Environ. Prot. 149 (2021) 465–475, https://doi.org/10.1016/j.psep.2020.11.022.
[44] M. Sánchez-Cantú, L.M. Pérez-Díaz, I. Pala-Rosas, E. Cadena-Torres, L. Juárez-Amador, E. Rubio-Rosas, M. Rodríguez-Acosta, J.S. Valente, Hydrated lime as an effective heterogeneous catalyst for the transesterification of castor oil and methanol, Fuel 110 (2013) 54–62, https://doi.org/10.1016/j.fuel.2012.07.075.
[45] M.-Y. Chen, J.-X. Wang, K.-T. Chen, B.-Z. Wen, W.-C. Lin, C.-C. Chen, Transesterification of soybean oil catalyzed by calcium hydroxide which obtained from hydrolysis reaction of calcium carbide, J. Chinese Chem. Soc. 59 (2012) 170–175, https://doi.org/10.1002/jccs.201100182.
[46] M. Sánchez-Cantú, L.M. Pérez-Díaz, R. Rosales, E. Ramírez, A. Apreza-Sies, I. Pala-Rosas, E. Rubio-Rosas, M. Aguilar-Franco, J.S. Valente, Commercial hydrated lime as a cost-effective solid base for the transesterification of wasted soybean oil with methanol for biodiesel production, Energy Fuels 25 (2011) 3275–3282, https://doi.org/10.1021/ef200555r.
[47] K. Piekarska, M. Sikora, M. Owczarek, J. Jóźwik-Pruska, M. Wiśniewska-Wrona, Chitin and chitosan as polymers of the future—obtaining, modification, life cycle assessment and main directions of application, Polymers (Basel) 15 (2023) 793, https://doi.org/10.3390/polym15040793.
[48] A.C. Egil, B. Ozdemir, S.K. Gunduz, M. Altıkatoglu-Yapaoz, Y. Budama-Kilinc, E. Mostafavi, Chitosan/calcium nanoparticles as advanced antimicrobial coating for paper documents, Int. J. Biol. Macromol. 215 (2022) 521–530, https://doi.org/10.1016/j.ijbiomac.2022.06.142.
[49] E. Guibal, Interactions of metal ions with chitosan-based sorbents: a review, Sep. Purif. Technol. 38 (2004) 43–74, https://doi.org/10.1016/j.seppur.2003.10.004.
[50] C.-C. Fu, T.-C. Hung, C.-H. Su, D. Suryani, W.-T. Wu, W.-C. Dai, Y.-T. Yeh, Immobilization of calcium oxide onto chitosan beads as a heterogeneous catalyst for biodiesel production, Polym. Int. 60 (2011) 957–962, https://doi.org/10.1002/pi.3031.
[51] H. Kayser, F. Pienkoß, P. Domínguez de María, Chitosan-catalyzed biodiesel synthesis: proof-of-concept and limitations, Fuel 116 (2014) 267–272, https://doi.org/10.1016/j.fuel.2013.08.013.
[52] D. KNORR, Functional properties of chitin and chitosan, J. Food Sci. 47 (1982) 593–595, https://doi.org/10.1111/j.1365-2621.1982.tb10131.x.
[53] A. Dhakshinamoorthy, M. Jacob, N.S. Vignesh, P. Varalakshmi, Pristine and modified chitosan as solid catalysts for catalysis and biodiesel production: a minireview, Int. J. Biol. Macromol. 167 (2021) 807–833, https://doi.org/10.1016/j.ijbiomac.2020.10.216.
[54] A. Wang, W. Quan, H. Zhang, Efficient synthesis of biodiesel catalyzed by chitosan-based catalysts, Int. J. Chem. Eng. (2021) 2021, https://doi.org/10.1155/2021/8971613.
[55] R.A. Lusiana, R. Nuryanto, D. Dayanti, Khabibi, N. Wijayati, N.A. Sasongko, A. R. Wijaya, Synthesis and characterization of chitosan/polyvinyl alcohol immersed in sodium hydroxide thin film as a heterogeneous catalyst in biodiesel production, Int. J. Biol. Macromol. 251 (2023) 126378, https://doi.org/10.1016/j.ijbiomac.2023.126378.
[56] I.P. Cantika, M.A. Zulfikar, H. Rusli, Synthesis of ethylenediamine modified chitosan beads for biodiesel production catalyst: a preliminary study, J. Kim. Sains Dan Apl. 26 (2023) 230–237. https://ejournal.undip.ac.id/index.php/ksa/article/view/55988.
[57] S. Prabakaran, K.J. Rupesh, I.S. Keeriti, S. Sudalai, G. Pragadeeswara Venkatamani, A. Arumugam, A scientometric analysis and recent advances of emerging chitosan-based biomaterials as potential catalyst for biodiesel production: a review, Carbohydr. Polym. 325 (2024) 121567, https://doi.org/10.1016/j.carbpol.2023.121567.
[58] M. Ambrosi, L. Dei, R. Giorgi, C. Neto, P. Baglioni, Colloidal particles of Ca(OH) 2 : properties and applications to restoration of frescoes, Langmuir 17 (2001) 4251–4255, https://doi.org/10.1021/la010269b.
[59] H. Espinosa-Andrews, O. Sandoval-Castilla, H. Vázquez-Torres, E.J. Vernon-Carter, C. Lobato-Calleros, Determination of the gum Arabic–chitosan interactions by Fourier Transform Infrared Spectroscopy and characterization of the microstructure and rheological features of their coacervates, Carbohydr. Polym. 79 (2010) 541–546, https://doi.org/10.1016/j.carbpol.2009.08.040.
[60] M.C. Sportelli, A. Volpe, R.A. Picca, A. Trapani, C. Palazzo, A. Ancona, P. Lugarà, G. Trapani, N. Cioffi, Spectroscopic characterization of copper-chitosan nanoantimicrobials prepared by laser ablation synthesis in aqueous solutions, Nanomaterials 7 (2016) 6, https://doi.org/10.3390/nano7010006.
[61] I. Galan, F.P. Glasser, D. Baza, C. Andrade, Assessment of the protective effect of carbonation on portlandite crystals, Cem. Concr. Res. 74 (2015) 68–77, https://doi.org/10.1016/j.cemconres.2015.04.001.
[62] NIST XPS Database, (2000). https://srdata.nist.gov/xps/main_search_menu.aspx.
[63] I. Corazzari, R. Nisticò, F. Turci, M.G. Faga, F. Franzoso, S. Tabasso, G. Magnacca, Advanced physico-chemical characterization of chitosan by means of TGA coupled on-line with FTIR and GCMS: thermal degradation and water adsorption capacity, Polym. Degrad. Stab. 112 (2015) 1–9, https://doi.org/10.1016/j.polymdegradstab.2014.12.006.
[64] Z. Mirghiasi, F. Bakhtiari, E. Darezereshki, E. Esmaeilzadeh, Preparation and characterization of CaO nanoparticles from Ca(OH)2 by direct thermal decomposition method, J. Ind. Eng. Chem. 20 (2014) 113–117, https://doi.org/10.1016/j.jiec.2013.04.018.
[65] L. Zeng, C. Qin, L. Wang, W. Li, Volatile compounds formed from the pyrolysis of chitosan, Carbohydr. Polym. 83 (2011) 1553–1557, https://doi.org/10.1016/j.carbpol.2010.10.007.
[66] M. Sánchez-Cantú, F.M. Reyes-Cruz, E. Rubio-Rosas, L.M. Pérez-Díaz, E. Ramírez, J.S. Valente, Direct synthesis of calcium diglyceroxide from hydrated lime and glycerol and its evaluation in the transesterification reaction, Fuel 138 (2014) 126–133, https://doi.org/10.1016/j.fuel.2014.08.006.
[67] R. Ezzati, S. Ranjbar, A. Soltanabadi, Kinetics models of transesterification reaction for biodiesel production: a theoretical analysis, Renew. Energy. 168 (2021) 280–296, https://doi.org/10.1016/j.renene.2020.12.055.
[68] J.J. Carberry, Physico-chemical aspects of mass and heat transfer in heterogeneous catalysis. Catalysis, Springer Berlin Heidelberg, Berlin, Heidelberg, 1987, pp. 131–171, https://doi.org/10.1007/978-3-642-93278-6_3.
[69] A. Talebian-Kiakalaieh, N.A.S. Amin, H. Mazaheri, A review on novel processes of biodiesel production from waste cooking oil, Appl. Energy. 104 (2013) 683–710, https://doi.org/10.1016/j.apenergy.2012.11.061.
[70] K. Hanisah, S. Kumar, A. Tajul, The Management of waste cooking oil: a preliminary survey, Heal. Environ. J. 4 (2013) 76–81. http://hej.kk.usm.my/pdf/HEJVol.4No.1/Article08.pdf.
[71] U. Klinkesorn, The role of chitosan in emulsion formation and stabilization, Food Rev. Int. 29 (2013) 371–393, https://doi.org/10.1080/87559129.2013.818013.
[72] P.C. Schulz, M.S. Rodríguez, L.F. Del Blanco, M. Pistonesi, E. Agulló, Emulsification properties of chitosan, Colloid Polym. Sci. 276 (1998) 1159–1165, https://doi.org/10.1007/s003960050359.
[73] W. Xia, P. Liu, J. Zhang, J. Chen, Biological activities of chitosan and chitooligosaccharides, Food Hydrocoll. 25 (2011) 170–179, https://doi.org/10.1016/j.foodhyd.2010.03.003.